Inclusion of eddy-currents impact in the model of a switched reluctance machine based on the equivalent electric circuit

J. Corda and S. M. Jamil

School of Electronic and Electrical Engineering
University of Leeds
Leeds, LS2 9JT (United Kingdom)
Phone: +44 113 3432045, Fax::+44 113 3432032, e-mail: **j.corda@leeds.ac.uk**

Abstract. The paper outlines a method for inclusion of the impact of eddy-currents in the model for dynamic prediction of current waveform and force of a switched reluctance machine. The method is based on the equivalent electric circuit model which accounts for the impacts of magnetic saturation and eddy currents in the magnetic core. A linear tubular switched reluctance machine, which includes solid steel elements in the magnetic core, is selected for a case study.

Key words

Switched-reluctance, motors, inductance, saturation, eddy-currents, losses

1. Introduction

Phase windings of a switched reluctance (SR) machine are supplied with unipolar voltage pulses from power electronic converter which operates either in a single-pulse or a current chopping/p.w.m. mode. The resulting flux waveforms in the machine are principally determined by the magnitude of the supply voltage, pulse widths and the switching frequency. The flux variations in time [1]-[2] have various levels of complexity in different parts of the magnetic core and can cause substantial iron losses. An example of flux variations in various parts of the core of a rotary four-phase SR machine, when it operates in a 'single-pulse' excitation mode, is illustrated in Fig.1.

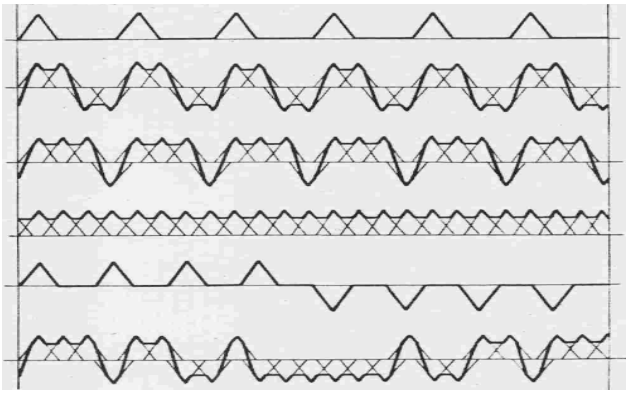

Fig. 1. Flux waveforms of a rotary four-phase SR machine [1].

The modelling of the core losses in a rotary SR machine, which is based on the available magnetic circuit characteristics and geometric parameters, had been dealt with in several publications, e.g. [3]-[6]. Such models are used in the process of electromagnetic design. However, the development of the control algorithm for a physically available SR machine is normally carried out using a model which relies on the machine's electrical equivalent circuit. Due to the complexity of flux waveforms, the representation of the eddy-currents and hysteresis effects through an equivalent circuit is quite intricate.

This paper outlines how the effect of iron losses in the magnetic core is accounted for in predicting the phase current waveform and force of a SR machine and what implications it has on its mechanical characteristic. A linear tubular 4-phase SR machine with the stator core diameter 80 mm and the core length 106 mm [7] is selected for a case study. Such a machine incorporates solid (non-laminated) steel elements in the magnetic core, which gives an enhanced rise of eddy-currents and hence the core losses.

2. Per-Phase Equivalent Circuit Parameters

The per-phase equivalent circuit of SR machine is shown in Fig.2. For the analysis of the machine with insignificant core losses, the representation by an

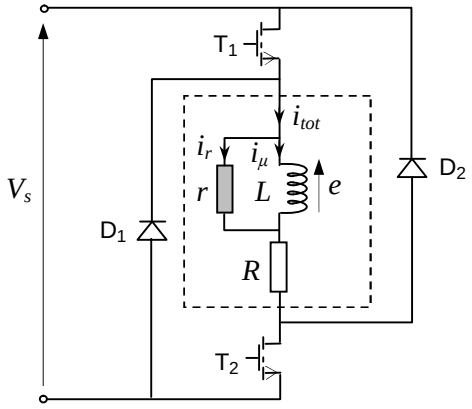

Fig. 2. Functional per-phase equivalent circuit of SR machine.

approximate equivalent circuit which includes the winding resistance (R) and the self-inductance (L) as a nonlinear circuit element is usually sufficient. However, if the core losses are significant, the representation requires inclusion of either a cascaded circuit network [8] or a lumped nonlinear multi-variable resistance (r) connected in parallel with the self-inductance [9].

The self-inductance (L) and the equivalent resistance representing the core losses (r), here from referred as the 'equivalent iron-loss resistance', are non-linear multivariable parameters. L is dependent on the instantaneous current (i) and position (x), while r is dependent on the instantaneous rate of flux linkage change (which in turn is determined by the instantaneous phase current at a given supply voltage), position and frequency of switching (f_{sw}).

If the of phase voltage differential equations of SR machine are expressed in explicit form in terms of phase currents, which might seem appropriate for applying standard routines for their numerical integration, this would necessitate introduction of coefficients which are partial derivatives of the non-linear inductance variation. The errors introduced by fitting the curves to describe the variation of L vs. position and current are increased by the process of differentiation, and this in turn results in substantial errors in predicting the waveform of instantaneous current and the force. For this reason an alternative method for solving the voltage differential equations in implicit form, which does not require the evaluation of differential coefficients, was developed and originally described in [10]. For the convenience of integrating the equations by this method, the magnetisation characteristics of SR machine are expressed through the flux linkage (ψ), rather than inductance. (The inductance is related to the flux linkage through the simple relationship $L = \psi / i$.) The magnetisation characteristics are measured by the method described in [9] for a range of locked positions and are shown in Fig.3.

In addition to the magnetisation characteristics, the model of SR machine, which is based on the equivalent

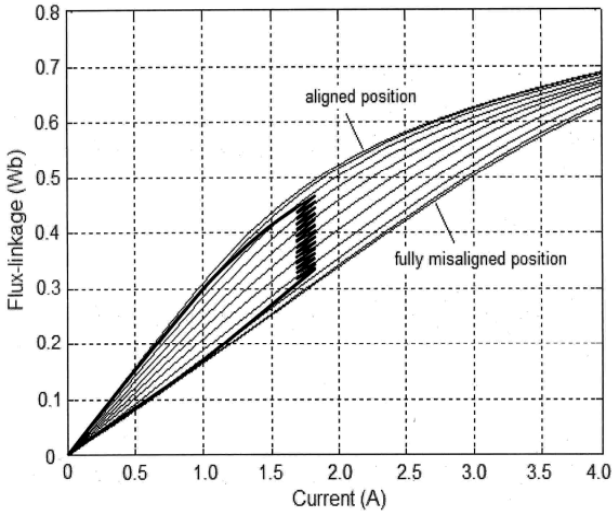

Fig. 3. Magnetisation characteristics.

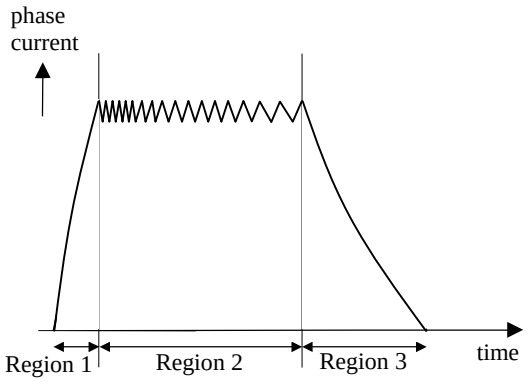

Fig. 4. Typical phase current waveform of linear SR motor.

circuit (Fig.2), uses the equivalent iron-loss resistance characteristics which are derived from measurements carried out also under *static* conditions.

In the running state at a given voltage, the instantaneous phase current determines the rate of flux-linkage change which is associated with eddy-current losses. A typical phase current waveform of a linear SR machine, running as a motor, is illustrated in Fig.4 and the corresponding locus of flux-linkage vs. current is indicated by a thick line in Fig.3. There are three distinctive regions: (R1) the rising interval during which both switches are in ON state, and the mover poles are passing from a misaligned position into a fractional overlap with the stator poles, (R2) the chopping interval imposed by the hysteresis controller during which one switch is chopping and the other one is in ON state, and the mover poles are fractionally overlapped with the stator poles and (R3) the decaying interval during which both switches are in OFF state, and the mover poles are approaching and possibly passing the aligned position. The flux-linkage rises during regions R1 and R2, though it ripples in region R2, and it decays during region R3.

The equivalent iron-loss resistance characteristics, which are related to the rising and decaying intervals (excluding the chopping) of the flux-linkage variation in the model, are derived from measurements carried out by applying the pulse of duration required to build up the current to a desired level at a given supply d.c. voltage, as

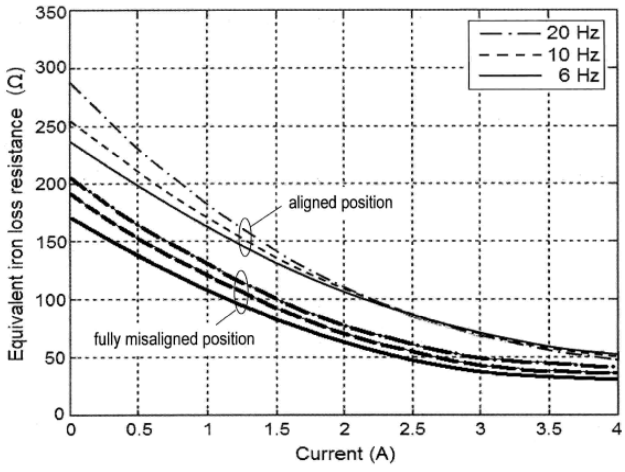

Fig. 5. The 'equivalent iron-loss resistance' characteristics used for the rising and decaying flux regions.

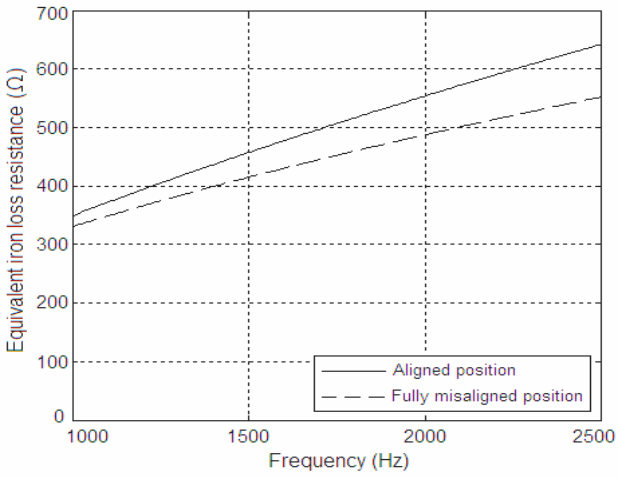

Fig. 6. The 'equivalent iron-loss resistance' characteristics used for the chopping region.

described in [9]. The measurements are repeated at several levels of currents while the mover is locked first in the aligned and subsequently in the fully misaligned position. These characteristics are shown in Fig.5.

The equivalent iron-loss resistance characteristics, which are related to the chopping interval in the model, are derived from measurements carried out by applying a.c. current with the peak-to-peak magnitude equal to the hysteresis band of chopping, as described in [9]. The measurements are repeated at several levels of high frequencies while the mover is locked first in the aligned and subsequently in the fully misaligned position. These characteristics are shown in Fig.6.

The equivalent iron-loss characteristics at intermediate positions are approximated by linear interpolations.

3. Model with Core Losses

Based on the equivalent circuit (Fig.2), the phase circuit equations are expressed as:

$$\frac{d\psi(i_\mu, x)}{dt} = v - R \cdot i_{tot} - \Delta v_{semicon} \qquad (1)$$

$$i_{tot} = i_\mu + i_r \qquad (2)$$

$$i_r = \frac{1}{r} \cdot \frac{d\psi(i_\mu, x)}{dt} \qquad (3)$$

where

$$v = \begin{cases} +V_s & \text{when both transistors are ON} \\ 0 & \text{when one transistor is ON and the other is OFF} \\ -V_s & \text{when both transistors are OFF} \end{cases}$$

x denotes instantaneous position.

The force produced by one phase at the instantaneous current i is computed as:

$$F(x,i) = \frac{\partial}{\partial x} \int_0^i \psi(i_\mu, x)\, d i_\mu \qquad (4)$$

The total force is computed by superposition of component forces of individual phases, i.e.:

$$F(x) = \sum_{k=1}^{4} F(x, i_{(k)}) \qquad (5)$$

[Assuming symmetrical phases and a quasi-steady state running (constant speed), the waveforms of individual phase currents i_1, i_2, i_3, and i_4 are sequentially shifted from each other for $\pi/2$ electrical degrees, i.e. position-wise by a quarter of the mover pitch.]

The total average force can be computed either by averaging the waveform of instantaneous force over the mover pitch length (λ), or from the area of the locus of flux-linkage vs. current in Fig.3, i.e.:

$$F_{avr} = \frac{4}{\lambda} \oint \psi \, d i_\mu \qquad (6)$$

The flow-chart of SR machine model which includes impact of core losses on the waveform current and the force through equivalent electric circuit is outlined in Fig.7. The magnetisation characteristics and the equivalent iron loss characteristics for the rising and decaying intervals, as well as for the chopping interval, are used as input data in the form of look-up tables referred to as $\psi(i_\mu, x)$, $r(i_\mu, x, f_{sw})$ and $r(f_{ch}, x)$, respectively.

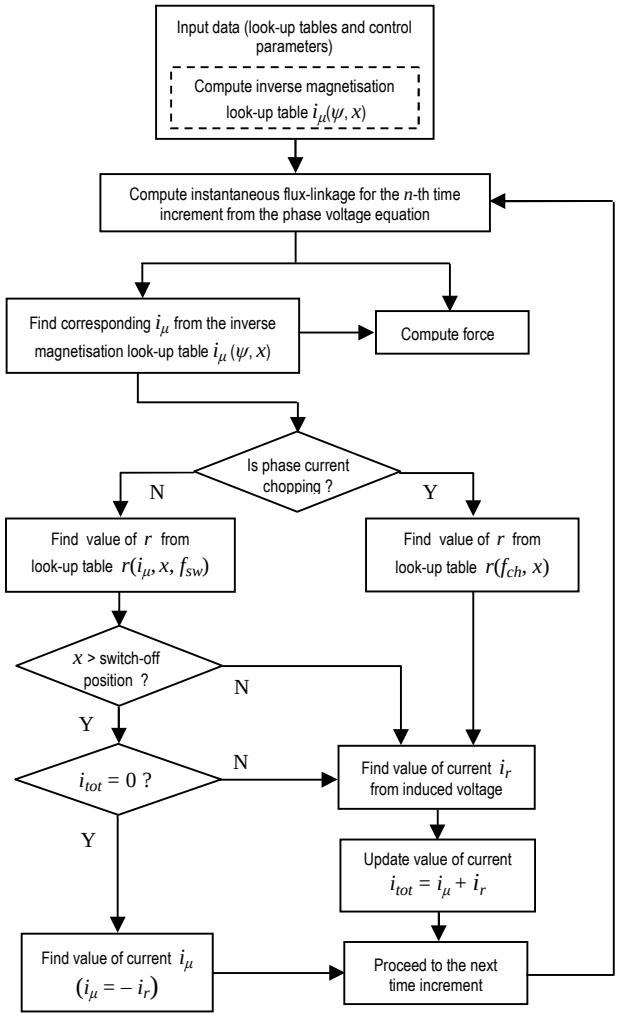

Fig. 7. Outline of the flow-chart of SR machine model showing the detail related to the inclusion of eddy-current effect.

Numerical integration of nonlinear equations (1) - (3) is carried out using the method described in [10] and applying it to the magnetising current component i_μ. The iron-loss current component i_r is found from the instantaneous rate of the flux-linkage change and the equivalent iron-loss resistance characteristics. The sum of these two current components gives the total instantaneous phase current, which is controlled by the main switching positions and chopping.

During hysteresis chopping current control (Region 2 in Fig.4), the chopping frequency varies due to the variation of inductance with position. The equivalent iron-loss resistance for a particular chopping cycle is therefore determined on the basis of the frequency estimated from the precursor cycle.

A sample of one cycle of the phase current and induced e.m.f. waveforms, under steady-state running condition, is shown in Fig.8. The current components i_μ and i_r are shown in Fig.9. An interesting effect is observed upon the phase (winding) current falls to zero and the diodes stop conduction. Despite the current is vanished, there is still induced e.m.f. in the phase coil. This is caused by a prolonged decay of flux which is supported by eddy currents in the core. Using the equivalent circuit of Fig.2 and applying $i_{tot} = 0$, i.e. $i_\mu = - i_r$ yields:

$$i_\mu = -\frac{1}{r} \cdot \frac{d\psi(i_\mu, x)}{dt} \qquad (7)$$

Hence the quantification of the flux decay immediately upon the phase (winding) current becomes zero is governed by the equivalent iron-loss resistance $r(i_\mu, x)$ and the magnetising characteristics $\psi(i_\mu, x)$.

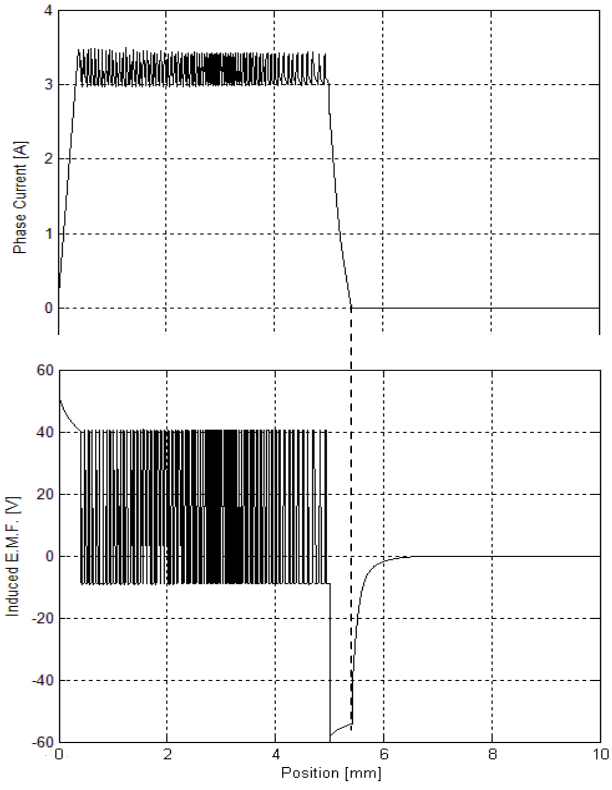

Fig. 8. Waveforms of phase current (i_{tot}) and induced e.m.f.

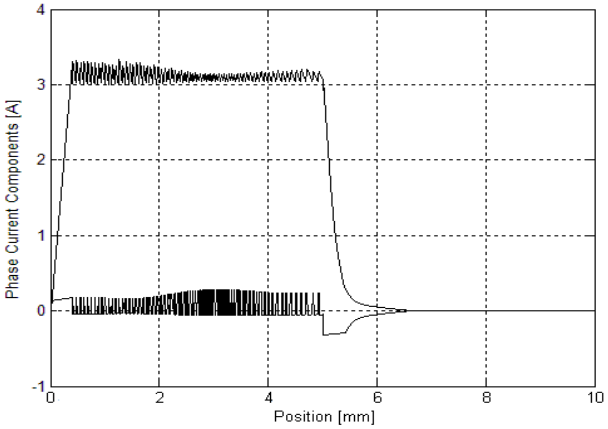

Fig. 9. Waveforms of phase current components i_μ and i_r.

The experimental evidence of this phenomenon is depicted in Fig.10 which relates to the same operating conditions as those applied for the prediction shown in Fig.9, i.e. at 50 V d.c. supply voltage, 3.2 A chopping current and 85 mm/sec operating speed.

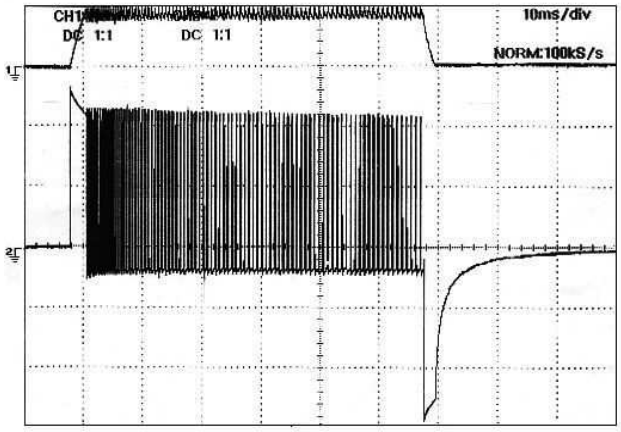

Fig. 10. Oscilloscope traces of phase current and induced e.m.f. (The latter is measured on the search coil which is wound in bifilar fashion with the main coil.)

4. Force v.s. Speed Characteristic

A bulk quantification of the impact of eddy-currents on the mechanical haracteristic is made by comparing the force vs. speed characteristics of the actual machine and a hypothetical counterpart machine without core losses. The maximum averaged dynamic force, which the motor is capable to develop at the rated current when running at a steady state speed, is called the pull-out force. The characteristic which indicates how this force changes with speed, is used to define the level of the running force capability of the linear SR motor.

To predict the pull-out force at a given speed, the model is run for a range of switching positions at the rated current limit, and the averaged dynamic force is computed for each run. The pullout force is than obtained by searching for the maximum value in the stored array of computed values of averaged dynamic forces. This process is repeated at different speeds to obtain the pull-out force vs. speed characteristic.

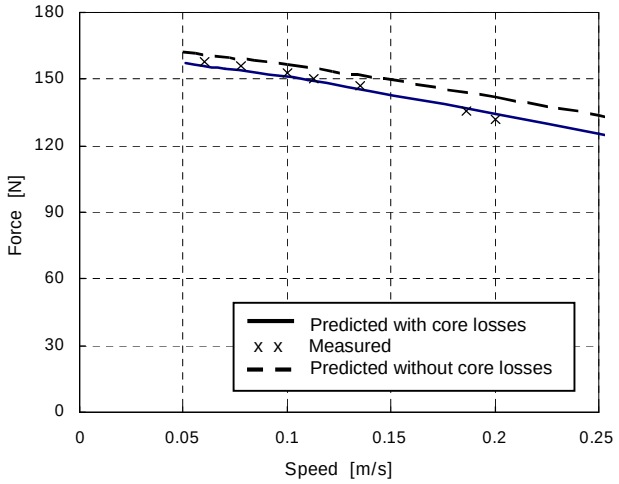

Fig. 11. The pull-out force vs. speed characteristics of the experimental linear-cylindrical SR motor for the phase current chopping limit of 3.2A.

As the pull-out force represents the level of load force required to be applied to the mover when running at a given speed to cause it to loose synchronism with the excitation, the tests for measurements of the pull-out force were carried out with the motor running in the open-loop switching mode at the rated current limit. While running at a constant speed (frequency), the machine was gradually loaded until the synchronism of the mover with excitation pulses was lost.

The pull-out force characteristic were predicted for the experimental linear-cylindrical SR machine (the stator core diameter 80 mm and the core length 106 mm [7]) by the model which includes impact of the core losses, and are is shown in Fig.11 along with results of measured force at several operating speeds.

In order to quantify the impact of core losses on the pull-out force characteristic, the prediction is also carried out by the model which does not include the impact of core losses. The corresponding characteristic is also shown in Fig.11.

The comparison of the characteristics related to the real machine (shown by solid line) with the one related to the hypothetical machine without core losses (shown by dashed line), indicates a reduction of pull-out force by 3.5% at the operating speed of 50 mm/sec, and by 6.5% at the speed of 250 mm/sec. At lower speeds the chopping region is dominant and the force reduction is smaller compared with the higher speeds where the force reduction is higher and is mainly caused by the core losses generated during the rising and decaying flux regions.

5. Conclusions

Using the equivalent electric circuit which describes the SR machine through the non-linear multi-variable parameters, which can be measured *statically*, the impact of core losses can be effectively included in the dynamic model for prediction of the machine performance. The eddy-currents generated in the magnetic core affect the current waveform, particularly at higher operating speeds where this effect causes a substantial deterioration of the output force.

References

[1] J. Corda, “Switched reluctance machine as a variable-speed drive”, Ph.D. Thesis, University of Leeds, U.K., 1979.

[2] P. J. Lawrenson, J. M. Stephenson, P. T. Blenkinsop, J. Corda, and N. Fulton, “Variable-speed switched reluctance motors”, IEE Proceedings – Pt.B, Vol.127, No.4, pp.253-265, 1980.

[3] A. Worley and J. M. Stephenson, “Eddy-current behavior in saturating laminations with impressed flux waveforms”, IEE Publication No.376, pp.229–233, 1993.

[4] J. Reinert, R. Inderka and R.W. De Doncker, “A novel method for the prediction of losses in switched reluctance machines”, Proc. of 7th European Conference on Power Electronis, Trondheim, Norway, pp.3608-3612, 1997.

[5] V. Raulin, A. Radun and I. Husain, “Modeling of losses in switched reluctance machines”, IEEE Transactions on Industry Applications, Vol.40, No.6, pp.1560-1569, 2004.

[6] J. T. Charton, J. Corda, J. M. Stephenson and S. P. Randall, “Dynamic modelling of switched reluctance machines with iron losses and phase interactions”, IEE Proceedings – Electric Power Applications, Vol.153, No.3, pp.327-336, 2006.

[7] J. Corda and E. Skopljak, “Linear switched reluctance actuator”, IEE Publication No.376, Oxford, U.K., pp.535-539, 1993.

[8] K. R. Geldhof, A.Van den Bossche, T. J. Vyncke and J. A. A. Melkebeek, “Influence of flux penetration on inductance and rotor position estimation accuracy of switched reluctance machines”, IEEE Conf. on Industrial Electronics, Taipei, Taiwan, pp.1246-1251, 2008.

[9] J. Corda and S. M. Jamil, “Experimental determination of equivalent circuit parameters of a tubular switched reluctance machine with solid-magnetic core”, IEEE Transactions on Industrial Electronics, Vol.57, No.1, pp.304-310, 2010.

[10] J. M. Stephenson and J. Corda, “Computation of torque and current in doubly salient reluctance motors from nonlinear magnetisation data”, IEE Proceedings, Vol.126, No.5, pp.393-396, 1979.